Hindawi
Aquaculture Research
Volume 2023, Article ID 9258423, 11 pages
https://doi.org/10.1155/2023/9258423

Research Article

The Fin-Improving Effects of Fucosylated Chondroitin Sulfate from Green and Purple *Apostichopus japonicus* on Caudal Fin Regeneration of Zebrafish Larvae

Tingting Hou,[1] Zaizhao Wang,[1] Kui Tang,[1] Shuai Zhang,[1] Shilin Liu,[2] Jialiang Liu,[3] Xiaoteng Fan,[1] and Xiaolin Liu [1]

[1]*College of Animal Science and Technology, Northwest A&F University, Yangling, Shaanxi 712100, China*
[2]*CAS Key Laboratory of Marine Ecology and Environmental Sciences, Institute of Oceanology Chinese Academy of Sciences, Qingdao 266071, China*
[3]*Shandong Oriental Ocean Science and Technology Company, Yantai, Shandong 264000, China*

Correspondence should be addressed to Xiaolin Liu; liuxiaolin@nwsuaf.edu.cn

Received 13 September 2022; Revised 9 October 2022; Accepted 4 November 2022; Published 11 February 2023

Academic Editor: Umit Acar

Copyright © 2023 Tingting Hou et al. This is an open access article distributed under the Creative Commons Attribution License, which permits unrestricted use, distribution, and reproduction in any medium, provided the original work is properly cited.

This study investigated the capability for fin regeneration in zebrafish larvae with the mechanism of FCS isolated from green and purple sea cucumbers *Apostichopus japonicus* (G-FCS and P-FCS). HPGPC determined that mean molecular weight of purified G-FCS and P-FCS is 19.5 and 18.8 kDa, and the FT-IR spectrum displayed similar characteristic absorption peaks. AFM images presented that G-FCS was shown as a spherical polysaccharide, while P-FCS molecules exhibited elongated chains. For the regeneration examination, FCS increased the regrowth area of the larval fin at 48 hours postamputation with enhanced locomotor behaviors, and the transcription levels of regeneration-related genes (*Wnt10a*, *msx1b*, *fgf20a*, *bmp2a*, *bmp4*, and *igf2b*) were upregulated. Moreover, FCS promoted the mRNA expression of inflammatory factors (*iNOS*, *TNF-α*, *IL-6*, *IL-10*, and *IFN-γ*) and TLR/NF-*κ*B pathway-related genes (*TLR3*, *TLR4a*, *NF-κb*, and *MyD88*). The Western blot analyses of TNF-*α* and IL-1*β* supported that FCS enhanced immune response. ELISA results indicated that FCSs increased the contents of NO, CAT, SOD, and G6PD. Summarily, the present results suggested that FCS was a potential regeneration enhancer by elevating immunomodulatory and antioxidative processes in zebrafish.

1. Introduction

The sea cucumber *Apostichopus japonicus* is considered one of the most valuable commercially farmed species in East Asia due to its abundant nutrition and medicinal properties [1], and the color of its body wall is an important factor that affects its taste and market price [2]. For example, the green color morph is the most common in nature, while the morph of purple individuals is scarce and regarded as a valuable species with high market potential [3, 4]. Several reports revealed that the biologically active extracts such as fucosylated chondroitin sulfates, the special form of polysaccharide in sea cucumber, have shown anticoagulant, antithrombotic, antiviral, antitumor, antioxidant, and immunomodulatory activities in vivo and in vitro [5]. Furthermore, a unique characteristic of sea cucumbers is that they could repair and regenerate themselves when injured, and the wound-healing properties of sea cucumber extracts also have been validated in animal models [6]. Additionally, the research on regeneration-promoting effects with the underlying mechanism of the specific FCS needs further clarification.

Wounding healing is a natural biological process involving in four overlapping stages including hemostasis, inflammation, proliferation, and remodeling [7]. These physiological phases should occur within a specific period in

the proper sequence for successful wound healing [8]. Meanwhile, various intrinsic factors such as complex cell signaling networks, numerous cell types, inflammatory mediators, oxidative stress, and growth factors were involved in promoting wound healing [9, 10]. Currently, the zebrafish (*Danio rerio*) serves as a fairly well-developed experimental model for regenerative and wound healing studies for its remarkable regenerative capacity in organs such as the kidney, heart, central nervous system, and appendages (fins) [11]. The fin regeneration had been intensively researched, and considerable progress had been made in revealing cellular and molecular mechanisms of potential regeneration for the fin. Further analysis of the precise function of these pathways had shown amazing complexity in the way they act [12]. Several signaling pathways were associated with fin regeneration, including fibroblast growth factor (FGF), bone morphogenic protein (BMP), insulin-like growth factor (IGF), hedgehog (Hh), Wnt/β-catenin, and nuclear factor-κB (NF-κB) [13].

Ample evidence supported that the immune system played a predominant role in the regeneration of injured tissue by clearing infectious and impaired cells, as well as initiating tissue repair [14–16]. This process heavily relies on the contribution of macrophages, which induced the clearing of cellular debris, deposition of the extracellular matrix (ECM), and synthesis of various growth factors and cytokines in the repair and restoration of tissue homeostasis [17]. Many botanical polysaccharides are endowed with the activation capability on macrophages, which is achieved through the combination of pattern recognition receptors (PRRs) including toll-like receptors (TLRs), scavenger receptors, and complement receptors [18]. In addition, oxidative stress is also thought as a key factor that could prevent the repairing of the wound with enormous free radicals impairing surrounding tissues [19]. In recent years, a number of natural biologically active substances with immunomodulatory, antimicrobial, antioxidant, or analgesic activities that had demonstrated biological and medicinal properties on wound healing [20, 21].

In the present study, FCSs from green and purple *A. japonicus* were purified and characterized to investigate their effects on wound healing and regeneration in the zebrafish larvae with caudal fin amputation. Besides, the potential mechanism of the regeneration-promoting capacity of FCS was clarified by examining the transcriptional response of regeneration signaling pathway-related genes, immunomodulatory activity, and antioxidative activity. The results would provide novel insight that FCS is a potential clinical medicine for therapies of wound healing.

2. Materials and Methods

2.1. Isolation and Purification of Sea Cucumber Polysaccharides. The crude polysaccharides were extracted from fresh green and purple *A. japonicus* (Shandong Oriental Ocean Sci-Tech Co. Ltd., China) according to the method described previously [22]. Briefly, the body wall of sea cucumber was lyophilized, smashed, and homogenized and added with KOH under stirring at 60°C (pH = 8.5). Then, the powder was hydrolyzed with Diastase vera (EC 3.3.21.4) in sodium acetate buffer before centrifugation. The supernatants were precipitated with threefold 95% (v/v) ethanol. The precipitates were distilled and added with 1.5 M KOAc (4°C overnight) before centrifugation and dialysis. After lyophilization, the crude polysaccharides were collected.

The crude polysaccharides were purified by *Q* Sepharose Fast Flow column (300 mm × 30 mm) using the AKTApure (GE Healthcare, USA) system and were eluted with 0–2 mol/L linear gradient of NaCl at a flow rate of 1 mL/min. Fractions containing FCS were detected by the phenol/sulfuric method and then collected, dialyzed, and further purified on a Sephadex 25 column (100 cm × 2.6 cm) before lyophilized for subsequent analysis.

2.2. The Purity and Molecular Weight Analysis. The purity and molecular weight of FCS were determined by high-performance liquid gel permeation chromatography (HPGPC, Agilent Technologies, USA) on the Shimadzu GPC-20A (Shimadzu, USA) with a RID-20A refractive index detector (Shimadzu, USA), which was equipped with a TSK gel GMPWXL column (7.6 × 300 mm, TOSOH, Japan). The mobile phase was 0.1 mol/L $NaNO_3$ (containing 0.06% NaN_3) at a flow rate of 0.6 mL/min. The molecular weight of FCS was calculated according to the standard calibration curve by Shimadzu GPC software (Shimadzu, USA).

2.3. Characterization of the FCS. For the Fourier transform-infrared (FT-IR) spectroscopy, the dried FCS was mixed with KBr (1 : 50) before being pressed to a transparent film and then scanned by Nicolet IS10 FT-IR spectrometer (Thermo Electron, USA) in the frequency range of 400 to 4000 cm^{-1}.

The molecular morphology of FCS was inspected using atomic force microscopy (AFM, Dimension Icon, Germany); the FCS solution (5 μg/mL in distilled water, 10 μL) was dropped onto freshly cleaved mica substrate and allowed to dry at room temperature (RT) for 24 h. Then, the samples were mounted on the AFM stage and acquired under tapping mode in ambient conditions at 25°C.

2.4. Zebrafish Husbandry and Embryo Collection. The wild-type AB zebrafish were purchased from the China Zebrafish Resource Center (Wuhan, China). Adult zebrafish were reared at 28 ± 1°C with a 14/10 h light/dark photoperiod and fed with brine shrimp twice a day. For fertilization, male and female zebrafish (1 : 1) were maintained together overnight. The fertilized and well-developed embryos were collected and maintained in an E3 embryo medium (EM) containing 0.2 mmol/L N-Phenylthiourea (PTU) (Aladdin, China) to prevent pigment formation. All investigations were approved by the regulations on experimental animals of Management methods of Laboratory Animals in Shaanxi Province, China (No. 150, 2011) and the Animal Ethics Committee of Northwest A&F University, Yangling, Shaanxi, China.

2.5. Caudal Fin Amputation and Drug Treatment for Zebrafish Larvae. At 72 hours postfertilization (hpf), larvae were anesthetized with 0.2 mg/mL tricaine (ethyl 3-aminobenzoate methanesulfonate, Aladdin, China). Then, the amputation of the caudal fin was performed using a sterile surgical blade and the pigment gap was considered as a reference. Following injury, larvae were placed in 6-well plates containing only dechlorinated water (A group) or water embracing G-FCS (100 μg/mL green-fucosylated chondroitin sulfate, G group) and P-FCS (100 μg/mL purple-fucosylated chondroitin sulfate, P group) immediately and maintained at 28°C for 4 h. Normal larvae without amputation (N group) were also anesthetized and recovered in the dechlorinated water as the control for wounding. Each treatment group was repeated four times. After that, all groups of zebrafish were transferred to dechlorinated water and maintained at 28°C.

2.6. Assessment of Fin Regeneration by Morphological Observation and Locomotor Behavior Assay. For morphological observation, the zebrafish were imaged immediately at 4, 24, 48, 72, 96, and 120 hours postamputation (hpa) under a microscope (Nikon, Japan). At least six images were captured for each group ($n = 4$). The tail regrowth area during wound healing was quantified with Image J 1.44 software (National Institutes of Health, USA).

The locomotor behavior assay was conducted according to the method described previously [23]. In brief, six larvae of each group were individually transferred in the 24-well plate with 2 mL culture water at 24, 48, and 72 hpa. After 10 min of acclimatization, larvae were recorded under visible light for 20 min by DaniorVision Observation Chamber (Noldus, Netherlands). The video data were analyzed using EthoVision XT (Noldus, Netherlands).

2.7. The Detection of NO, CAT, SOD, and G6PD Levels. In brief, the zebrafish larvae (twenty larvae per group, $n = 6$) were collected and rinsed with ice-cold PBS and homogenized with physiological saline using an ultrasonic processor (Sonics, USA). The level of nitric oxide (NO) and the activities of catalase (CAT), superoxide dismutase (SOD), and glucose-6-phosphate dehydrogenase (G6PD) were measured by corresponding assay kits (Nanjing Jiancheng Bioengineering Institute, China) following the manufacturer's protocols, respectively. After the reaction with the corresponding working solution, the absorbance at the respective wavelength was measured using a microplate reader (Bio Tek, USA). The contents or activities were calculated using the formulas according to the manual.

2.8. Quantitative Real-Time PCR (qRT-PCR) Analysis. At 4, 24, 48, and 72 hpa, twenty larvae per group ($n = 6$) were pooled and homogenized in TRIzol lysis reagent (TakaRa, China) for RNA extraction. The quality and quantity of RNA were checked by a nanodrop spectrophotometer (Thermo Electron Corporation, USA). The cDNA was synthesized by M-MLV reverse transcriptase (Invitrogen, USA) in a 20 μL volume containing 3 μg total RNA. The qRT-PCR was performed using an ABI Real-Time PCR system (Applied Biosystems, USA) and SYBR Green mix (TakaRa, China) following instructions. *β-actin* was used as the reference gene. The expressions of genes were determined by the cycle threshold (Ct) and the results were analyzed using the $2^{-\Delta\Delta CT}$ method. The sequences of the primers are listed in Table S1.

2.9. Western Blot Analysis. At 4, 24, 48, and 72 hpa, the larvae (twenty per group, $n = 6$) were collected and lysed using RIPA buffer (CWBIO, China) that contained protease inhibitors. The BCA protein assay kit (CWBIO, China) was used to detect the protein concentration. Protein samples were electrophoresed and transferred onto a polyvinylidene fluoride (PVDF) membrane (Millipore, USA). After block with 5% BSA (Bio-Rad, USA), the membrane was probed against the primary antibodies including anti-GAPDH (1 : 1000, ZSGB-BIO, China), anti-TNF-α (1 : 1000, Abcam, UK), and anti-IL-1β (1 : 1000, Cell Signaling Technology, USA) at 4°C overnight, subsequently incubated with corresponding secondary antibodies (1 : 2000, CWBIO, China) at RT for 2 h. After washing the remaining antibodies, enhanced chemiluminescence reagents (ECL, ZETA LIFE, USA) were used to capture the bands under the imaging system (Bio-Rad, USA). The bands were quantified by Image J 1.44 software. The expression of proteins was normalized to GAPDH.

2.10. Statistical Analysis. All data were performed through statistical analysis and shown as the mean ± standard error (SEM). The differences were analyzed with two-tailed *t*-tests or one-way analysis of variance (ANOVA) with Tukey's test using SPSS 20.0 software (SPSS, USA); $P < 0.05$ was considered statistically significant.

3. Results

3.1. Isolation and Purification of FCSs from Green and Purple A. Japonicus. After the extraction process, the yields of crude polysaccharides from green and purple *A. japonicus* were 5.78% and 5.33%, and the extraction efficiency was 53.32% and 51.90%, respectively. The fractions from green and purple *A. japonicus* crude polysaccharides that eluted with 0.66–0.71 and 0.63–0.77 mol/L NaCl were identified as FCSs. The contents and retention times in anion-exchange chromatography of the two FCSs were similar, indicating no significant difference in sulfate content. The yield of G-FCS and P-FCS from dried body walls was 0.95 and 1.30 mg/g, respectively, and FCS was more abundant in purple *A. japonicus*.

The purity and average molecular weights of purified FCSs were assessed by HPGPC; each fraction showed a single and symmetric peak that verified the homogeneity (Figure 1(a)). The retention time was 14.008 and 14.024 min, and the average molecular weights of G-FCS and P-FCS were figured out to be 19.5 and 18.8 kDa, respectively.

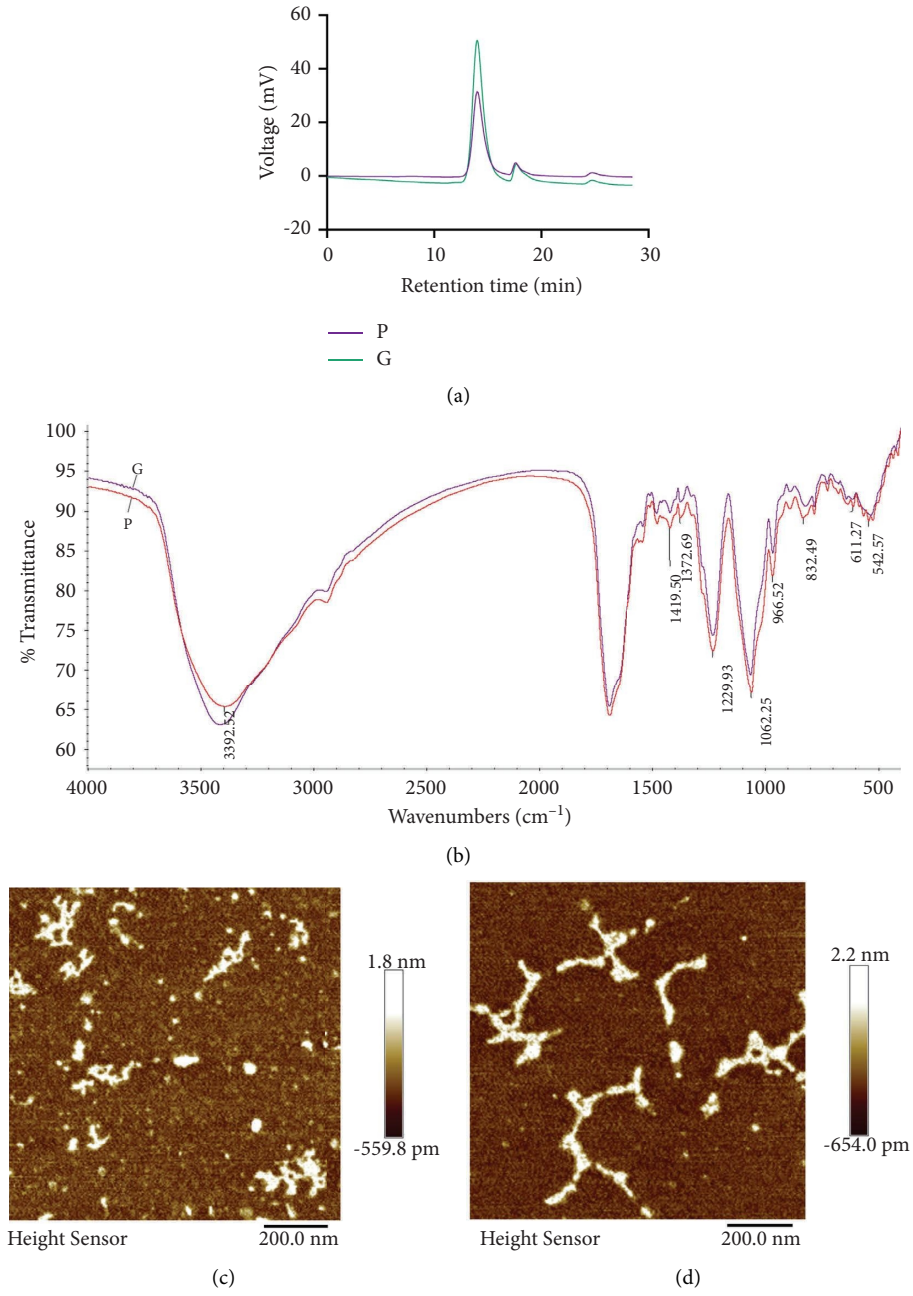

Figure 1: Purification and characterization of FCSs from green and purple *A. japonicus*. (a) HPGPC of G-FCS and P-FCS. (b) FT-IR spectrum of G-FCS and P-FCS from *A. japonicus*. The purple line indicates the FT-IR spectrum of G-FCS, and the red line indicates P-FCS. AFM images of (c) G-FCS and (d) P-FCS. Scale bar = 0.2 μm. G and P represent G-FUC and P-FUC, respectively.

3.2. FT-IR Spectrum and Morphological Characterization by AFM. To further identify FCSs, FT-IR spectra of two FCSs were analyzed between 4000 cm^{-1} and 400 cm^{-1} (Figure 1(b)), and the obtained spectrum presented similar characteristic absorption peaks. The signals at 3392 cm^{-1} and 1062 cm^{-1} were attributed to the stretching vibration of O–H and C–O, respectively. The bands at 2946 cm^{-1} were produced by the stretching vibration of C-H. The absorptions at 1062 cm^{-1} were derived from the asymmetric stretching vibration of C–O–C. The signals at 1229 cm^{-1} and 820–860 cm^{-1} were due to the vibration of S=O and C–O–S of sulfate, which confirmed the presence of sulfates in FCSs [24, 25]. The signal at 832 cm^{-1} indicated the presence of 6-*O*-sulfated-*N*-acteylgalactosammine and 2,4-*O*-disulfated fucose. These results confirmed that both FCSs were fucosylated chondroitin sulfates.

In addition, AFM was used to characterize surface conformation and obtain the thickness of macromolecular chains of FCSs. G-FCS was formed by the aggregation of random linear chains with a few spherical polysaccharide molecules in AFM images (Figure 1(c)), and the mean thickness was 1.8 nm while P-FCS molecules exhibited elongated chains (Figure 1(d)), whose thickness was measured at about 2.2 nm.

3.3. FCS Accelerated the Regeneration Program of Zebrafish Caudal Fin. To evaluate the healing ability of FCS, the tissue regeneration area of the tail fin after amputation in the 72 hpf zebrafish was measured. As shown in Figure 2(a), FCS treatment enhanced caudal fin tissue regeneration of zebrafish larvae after 24 hpa, and the amputated caudal fins were completely restored and exhibited a normal shape at 72 hpa. The quantified regeneration area of the caudal fin in the P-FCS treatment group was significantly larger than that G-FCS group and control group at 48 hpa ($P < 0.05$). And FCSs still had slight growth-promoting ability after caudal fin repair (Figure 2(b)). This observation indicated that 48 hpa was a key time point, which is essential for accelerating the healing process by FCS.

3.4. FCS Improved the Locomotor Activity of Zebrafish Larvae after Amputation. As the caudal fin plays a crucial role in fish locomotion, the motile behavior of zebrafish larvae after amputation was tracked at 24, 48, and 72 hpa to further explore the regeneration-promoting effects of FCS. P-FCS significantly increased the mean velocity, maximum acceleration, and total distance of movement at 24 hpa, as well as maximum acceleration at 48 hpa ($P < 0.05$), while there were no significant differences at other time points (Figures 3(a)–3(c)). Simultaneously, the cumulative duration of the mobile state and highly mobile state were also significantly prolonged, and that of the immobile state was correspondingly shortened at 24 hpa in the P-FCS treatment group ($P < 0.05$, Figures 3(d)–3(f)). Moreover, there was no significant difference in zebrafish larvae locomotor behaviors between the three groups at 48 and 72 hpa. These findings were in correspondence with the finding in Figure 2, which implicated that P-FCS shows regeneration-promoting potentials in zebrafish.

3.5. FCS Increased mRNA Expression of Regeneration-Related Genes. To further access the regeneration-promoting capabilities of FCS, the mRNA expressions of regeneration-related genes at 4, 24, 48, and 72 hpa were investigated. As shown in Figure 4, tail amputation increased *bmp2b* and *bmp4* gene expression in larvae at 24 and 72 hpa ($P < 0.05$). After G-FCS treatment, the expression level of *bmp4* at 24 hpa, muscle segment homeobox 1b (*msx1b*), and *bmp2a* at 48 hpa, *fgf20a*, *bmp2b,* and *bmp4* at 72 hpa were significantly increased ($P < 0.05$), while these genes expression at 4 hpa had no significant changes. In contrast, P-FCS significantly increased mRNA expressions of wingless-type MMTV integration site family, member 10A (*wnt10a*), *msx1b*, *fgf20a, bmp2a, bmp4*, and *igf2b* at 4 hpa, as well as *wnt10a*, *bmp2a,* and *bmp4* at 24 hpa ($P < 0.05$), whereas the expression of regeneration-related genes exhibited no significant difference at 48 and 72 hpa. These results indicated that G-FCS and P-FCS promote the regeneration program by upregulating the expression of regeneration-related genes at different times, and P-FCS responded faster in the healing process, which may account for the regrowth process of the larval fin (Figure 2).

3.6. FCS Activated the Immune Response in Larvae after Amputation. To investigate the mechanism of FCS in the tail fin regeneration process, the mRNA and protein expressions of pivotal cytokines in immune response, TLR-NF-κB signaling pathway-related genes, and the production of NO were detected. As shown in Figure 5(a), the mRNA expression of tumor necrosis factor α (TNF-α) and interleukin-6 (*il-6*) genes was markedly elevated following amputation; meanwhile, the protein expression of TNF-α was significantly increased (Figures 5(b) and 5(c), $P < 0.05$). G-FCS significantly increased the transcriptional level of *IL-6* and interferon-gamma 1 (IFN-γ), although the protein expression of TNF-α ($P < 0.05$) is inhibited; meanwhile, P-FCS significantly increased inducible nitric oxide synthase (*iNOS*), *TNF-α, IL-6*, *IL-10,* and *IFN-γ* genes expression levels, as well as promoted IL-1β protein level ($P < 0.05$). In addition, it was found that caudal fin amputation significantly suppressed the content of NO, while G-FSC and P-FCS inverted the inhibition of FCS in NO production, together with the dramatically enhanced NO level with P-FCS treatment that was consistent with the upregulation of *iNOS* ($P < 0.05$, Figures 5(a) and 5(d)). Among TLR-NF-κB signaling pathway-related genes, amputation increased the expression level of *NF-κb* ($P < 0.05$), while G-FCS treatment increased the gene expression levels of toll-like receptor 4a (*TLR4a*) and myeloid differentiation factor 88 (*MyD88*) ($P < 0.05$), and P-FCS showed a strong promoting effect on evaluating *TLR3*, *TLR4a*, *NF-κb,* and *MyD88* expressions (Figure 5(e)). These results revealed that FCS activated the immune response e following amputation, and P-FCS may have relatively stronger protection.

3.7. FCS Increased the Expression of Antioxidant Enzymes. To evaluate the effect of FCS on the maintaining of oxidative homeostasis in zebrafish after amputation, the antioxidant enzyme levels were detected. As shown in Figure 6, the contents of CAT, SOD, and G6PD were significantly decreased following amputation treatment, while G-FCS and P-FCS supplement both induced significant recovery ($P < 0.05$, Figure 6), indicating that FCS had the antioxidant capacity that may conquer the adversity.

4. Discussion

In the present study, two types of FCS were isolated from green and purple *A. japonicus*. There was little difference in molecular weight and functional groups between the two FCSs, while the discrepancy was found in the characterization of surface topological features. G-FCS was mainly composed of short linear chains with a few spherical lumps, indicating the molecular aggregation and the branched and entangled structures, which might be contributed to that the hydroxyl groups of FCS could form intimate interactions with each other [26]. Moreover, the 1.8 nm mean height of G-FCS was greater than that of the single-chain polysaccharides (0.1–1.0 nm), which suggested the formation of crosslinks between the G-FCS molecules. Similarly, FCS extracted from *Pearsonothuria graeffei* and *Isostichopus*

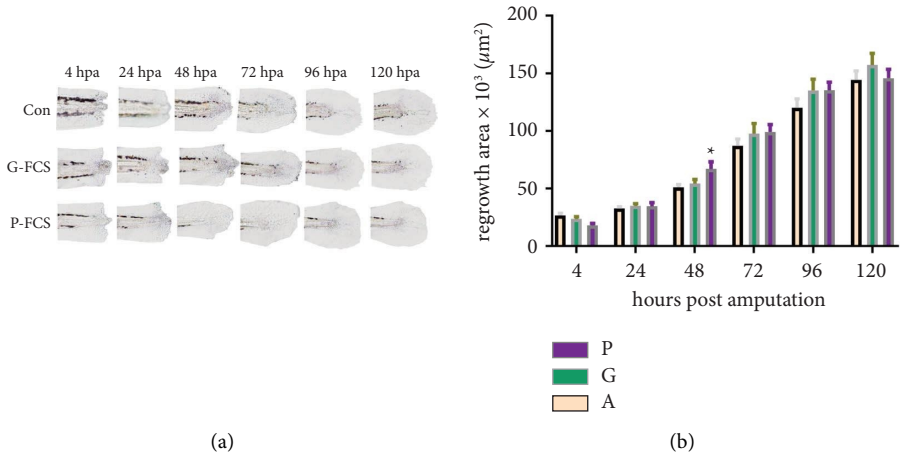

FIGURE 2: The effects of FCSs on fin regeneration of zebrafish larvae at 4–120 hpa. (a) The representative images show the zebrafish larvae fin regeneration under FCS treatment. (b) Quantitative analysis of the regrowth area of larvae fin ($n = 4$). The data are expressed as mean ± SEM and are analyzed by one-way of variance (ANOVA) followed by Tukey's test. The asterisk above columns signified significant differences among groups ($^*P < 0.05$). A, G, and P represent the amputation group, G-FCS treatment after amputation group, and P-FCS treatment after amputation group, respectively. The same as below.

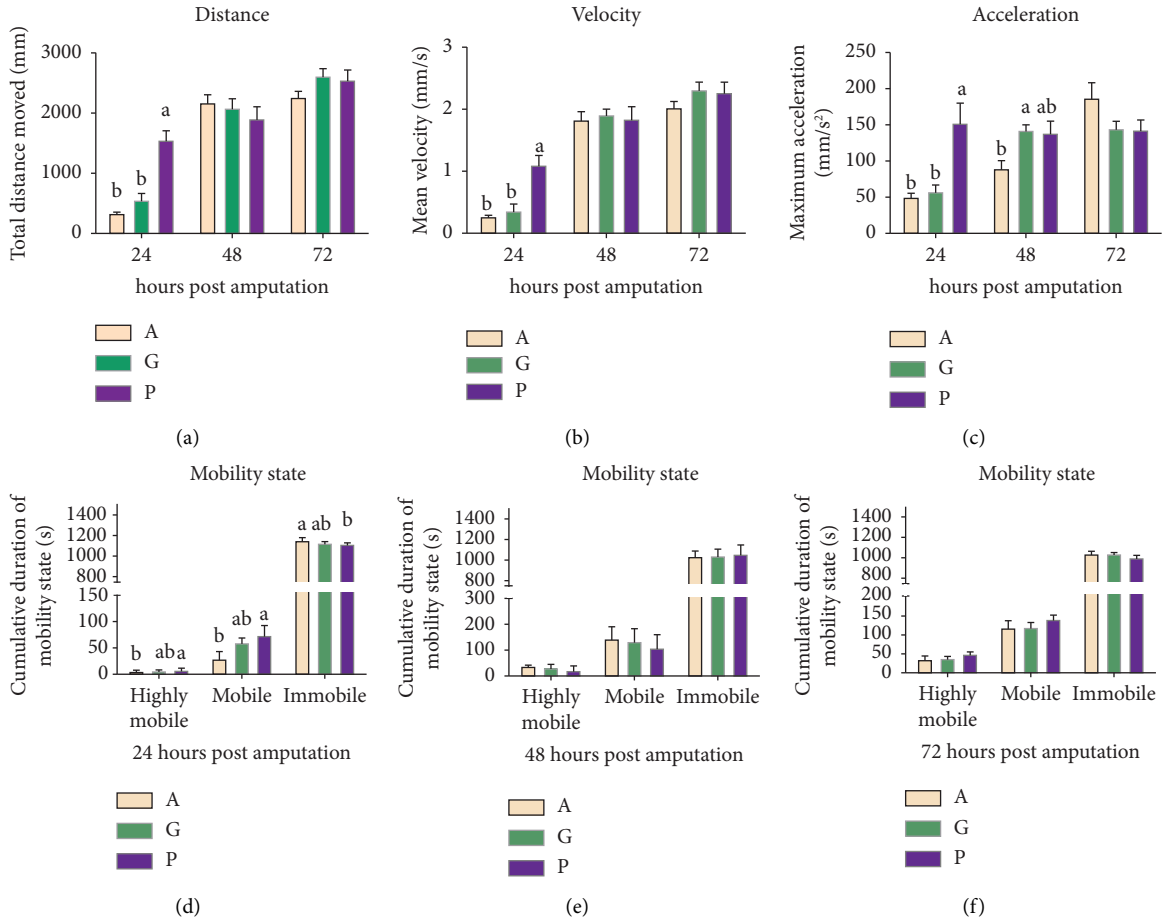

FIGURE 3: The effects of FCS on locomotor behaviors of zebrafish larvae at 24, 48, and 72 hpa. (a) The total distance of movement, (b) mean velocity, and (c) maximum acceleration at 24, 48, and 72 hpa. Cumulative duration of mobility state at 24 hpa (d), 48 hpa (e), and 72 hpa (f) ($n = 6$). The data are expressed as mean ± SEM and are analyzed by one-way of variance (ANOVA) followed by Tukey's test. Different small letters above columns signified significant differences among groups ($P < 0.05$).

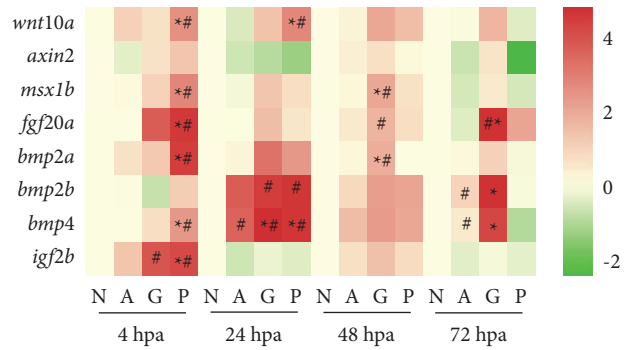

Figure 4: The effects of FCS on the mRNA levels of genes involved in the regeneration signaling pathway at 4, 24, 48, and 72 hpa. The average transcription values relative to the nonamputation zebrafish larvae at per time points are indicated by the color gradient and log2 transformed ($n = 6$). Hash signs signify a significant difference from the nonamputation zebrafish larvae based on two-tailed t-tests ($^{\#}P < 0.05$). Asterisks signify a significant difference from the corresponding only amputation group, determined by one-way analysis of variance (ANOVA) followed by Tukey's test ($^{*}P < 0.05$). N, A, G, and P represent normal larvae without amputation, the amputation group, G-FCS treatment after amputation group, and P-FCS treatment after amputation group, respectively. The same as below. *Wnt10a*, wingless-type MMTV integration site family, member 10A; *axin2*, axis inhibition protein 2; *msx1b*, muscle segment homeobox 1b; *fgf20a*, fibroblast growth factor 20a; *bmp2a/2b/4*, bone morphogenetic protein 2a/2b/4; *igf2b*, insulin-like growth factor 2b.

badionotus showed analogous structures [27]. While P-FCS molecules displayed elongated linear chains (Figure 1(d)), whose height of 2.2 nm is higher than the linear κ-carrageenan (0.66 ± 0.16) [28]. This phenomenon may be attributed to their branched structure that increased the steric hindrance of molecular chains. The conformation is similar to the FCS extracted from *A. japonicus* in previous research [29]. The biological activity of polysaccharides primarily counted on their structural features in which molecular weight and chain conformation are essentials that considerably influence the capacity of polysaccharides [30]. Therefore, the diversity of conformation between G-FCS and P-FCS could imply the diverse bioactivity properties they have.

Sea cucumber is regarded as a sort of functional food and pharmaceutical agent considering their unique capability of repairing, renewing, or regenerating themselves when damaged. Numerous research studies have revealed that extracts from sea cucumber benefited the wound healing process in various experimental animals [6], among which FCS as a unique type of polysaccharide existing in sea cucumber has shown therapeutic effects. The repair efficiency of FCS is exhibited in the central nervous system, liver development, and connective tissue [31]. In the present study, zebrafish larvae with amputated tails were used to explore the regeneration-promoting capability of FCS. Following amputation, the size and shape of the caudal fin of zebrafish larvae undergo a series of complex processes and are restored within 3 days, which is consistent with the observations in the previous study on zebrafish [32]. Compared to the control group, P-FCS significantly increased the regrowth area of the caudal fin at 48 hpa, explaining the events at 48 hpa were essential to promote wound closure. Meanwhile, both FCSs tend to facilitate the growth of zebrafish other than the initial period (within 4 hpa), which is coincident with the property of growth promotion for FCS extracted from *A. japonicus* on neurite in the previous investigation [33]. The locomotion of zebrafish larvae was affected by the caudal fin morphological impairment. Interestingly, the restoration of locomotor behavior was not always synchronous with the renewal of the caudal fin. Previous research found that the movement behavior of zebrafish larvae was restored at 48 hpa rather than at 72 hpa which could be the time point that the shape and size of the caudal fin were restored [34]. A similar phenomenon was discovered in this study that the movement behavior including total distance, maximum acceleration, and mean velocity of the P-FCS treatment group was significantly boosted at 24 hpa, other than the key time at 48 h that facilitate the restoration of the caudal fin. These observations demonstrated that P-FCS accelerated the recovery process of the movement behavior of zebrafish larvae and this change could attribute to the regeneration-promoting efficiency. Furthermore, the two FCSs promoted zebrafish larval fin regeneration to different degrees, and the P-FCS had a stronger promotion effect on caudal fin regeneration compared to the G-FCS, which might be attributed to the different molecular features.

Previous studies had demonstrated that there are multiple signaling pathways involved in caudal fin regeneration, such as Wnt/β-catenin, BMP, FGF, and IGF; these pathways generally synergistically regulate the regeneration process through complex coordinated mechanisms [12]. Our results found that the regeneration-related genes of zebrafish that were treated with FCSs were upregulated, manifesting that the promotion of fin regeneration caused by FCS may be the result of the intervention of these genes involved in regeneration. Similarly, the fucosylated chondroitin sulfate isolated from *Acaudina molpadioides* exhibited anti-adipogenic activity by enhancing the expression of the Wnt/β-catenin related factors [35]. FCS from *Holoturia Mexicana* showed strong binding affinities to fibroblast growth factors 1 and 2, suggesting the neovascularization promotion of FCS [36]. The exogenous chondroitin sulfate was proved to possess deep affinities to FGF and BMPs, oversulfated chondroitin sulfate-E improved osteoblast differentiation by binding to BMP4 [37, 38]. In addition, we found that there are temporal differences and target disparities for signal pathways, that P-FCS activated more regeneration-related genes and responded at an early stage, while G-PCS targeted *msx1b*, *fgf20a*, and BMP pathway-related genes in the later stages of caudal fin renewal. It is accorded with the morphological observations for promoted caudal fin regeneration and might account for that P-FCS prompted the regeneration of the fin at 48 hpa.

There is substantial evidence showing that the immune system played a key role in tissue regrowth and regeneration, which mitigated infections, cleared impaired cells, and initiated tissue repair [17, 39]. It had identified that TNF-α

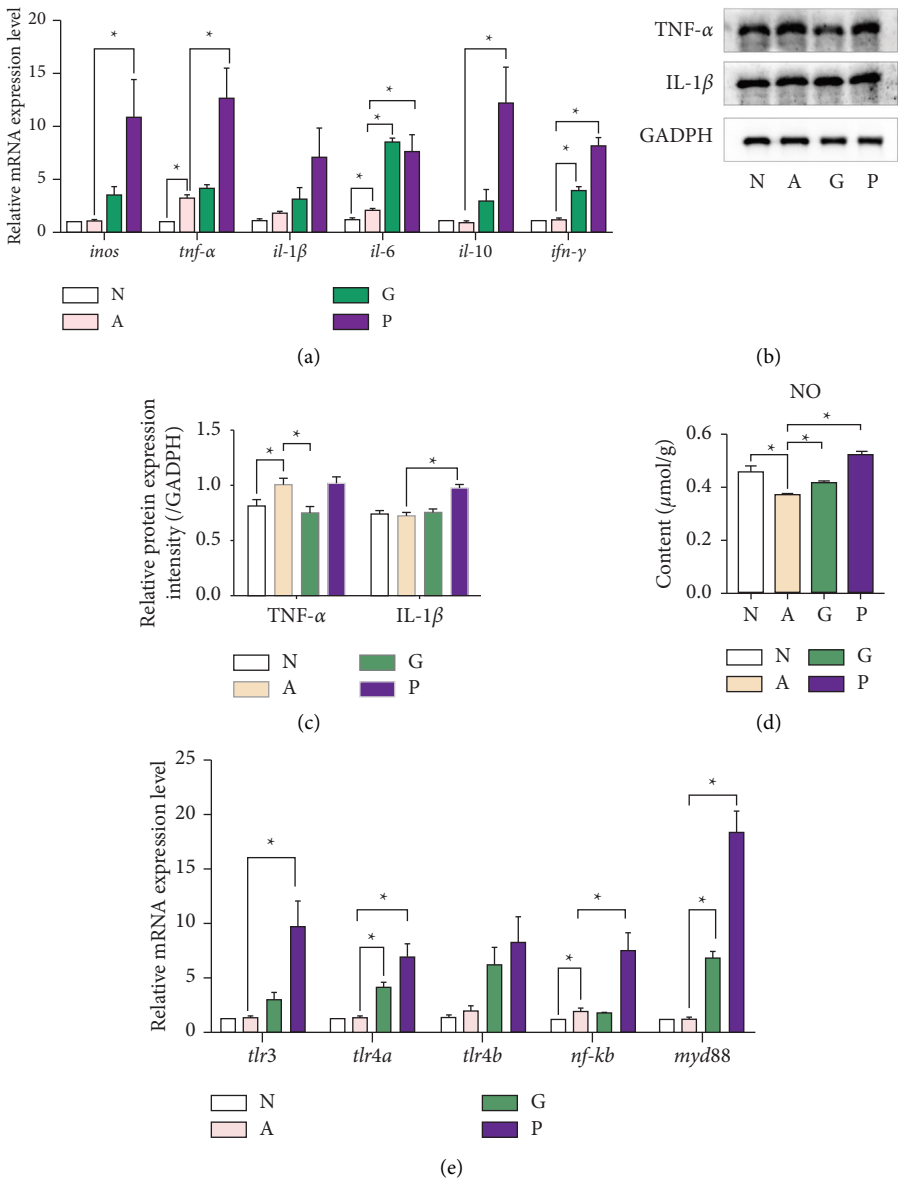

FIGURE 5: The effects of FCS on the immune response of zebrafish larvae at 48 hpa. (a) The transcription levels of genes related to the immune response. (b, c) Relative protein expression of TNF-α and IL-1β in zebrafish larvae evaluated by Western blot. (d) The contents of NO in zebrafish larvae. (e) The mRNA expression of TLR/NF-κB signaling pathway-related genes. All the experiments are conducted in triple ($n = 6$). The data are expressed as mean ± SEM. Asterisks signify a significant difference ($P < 0.05$). *iNOS*, inducible nitric oxide synthase; *TNF-α*, tumor necrosis factor *α*; *IL-1β/6/10*, interleukin-1*β*/6/10; *IFN-γ*, interferon-gamma 1; *TLR3/4a/4b*, toll-like receptor 3/4a/4b; *NF-κb*, nuclear factor-*κ*B; *MyD88*, myeloid differentiation factor 88.

was one of the key signals expressed transiently by macrophages during the early stages of regeneration, which controlled the regeneration process by inducing the inflammatory mediators [16]. The IL-1β-mediated transient inflammatory response was required for proper regeneration in the fin; it played a vital role in caudal fin regeneration by regulating the expression of regeneration-related genes [14]. Moreover, IL-10 was crucial for sar-free healing in fetal mice and adult mice that IL-10 overexpressed, which is likely due to the regulation of inflammation, as well as the extracellular matrix, fibroblast cell, and endothelial progenitor cells function [40]. It proved that FCS from *A. japonicus* exerted excellent immunomodulatory activities in both congenital and adaptive immune systems [41]. FCS from *Stichopus chloronotus* had been demonstrated to promote the pinocytic activity, the proliferation, and the production of cytokines and NO on RAW 264.7 cells, suggesting that FCS could enhance the immune response of macrophages [42]. Our research showed that cytokines-related genes were upregulated and both FCSs possessed the ability to regulate the proinflammatory cytokines including *TNF-α*, *IL-6*, and anti-inflammatory cytokine *IL-10* and *iNOS* expression associated with the production of NO for enhancing immunity. IFN-γ could trigger macrophages to release

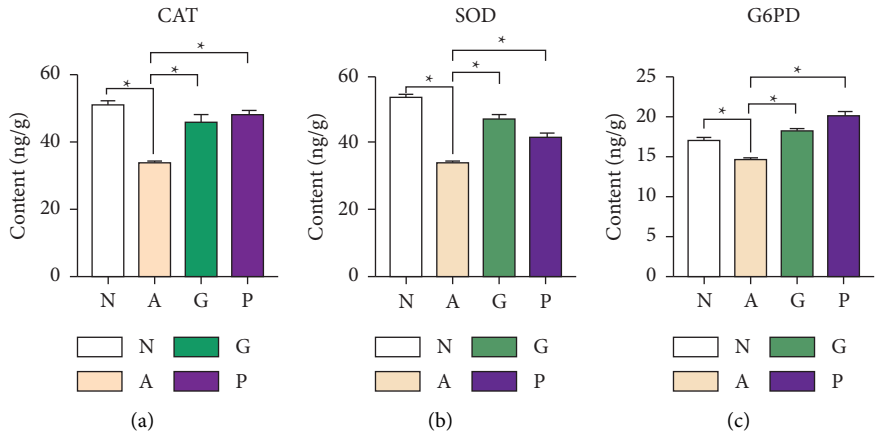

FIGURE 6: The effects of FCS on the protein expression of antioxidant enzymes of zebrafish larvae at 48 hpa. The contents of (a) CAT, (b) SOD, and (c) G6PD in zebrafish larvae following amputation ($n = 6$). The data are expressed as mean ± SEM. Asterisks signify significant differences ($P < 0.05$). CAT, catalase; SOD, superoxide; G6PD, glucose-6-phosphate dehydrogenase.

proinflammatory cytokines and produce increased amounts of nitrogen radicals, oxygen, and superoxide anions to enhance their killing capacity [43]. Present results of upregulated *IFN-γ* expression as well as the augmented protein expression of TNF-*α* and IL-1*β* proved the activation of immune response under FCS treatment, reflecting that FCSs had immunostimulatory effects on zebrafish caudal fin regeneration. Coincidentally, the glycosaminoglycan extracted from *Stichopus hermanii* was also showing positive effects on modulating inflammation in the healing process in rats with oral mucous traumatic ulcers [44].

Previous studies had reported that plant polysaccharides activated the macrophages' immune responses mainly through TLRs [45]. Both MyD88 dependent/independent TLR signaling pathways activate transcription factors such as NF-*κ*B by recognizing homologous ligands, sequentially a series of inflammatory cytokines and chemokines which were essential in immune responses also be mobilized [46, 47]. Among them, TLR4 was revealed to be effective in tissue repair and regeneration, and a slower healing process was found in TLR4$^{-/-}$ mice [48]. Besides, the TNF-*α*/TNFR1 signaling pathway is demanded for blastema cell proliferation and fin regeneration in zebrafish larvae [16]. In the present study, the mRNA expression of *TLR3*, *4a*, *myd88,* and *nf-κb* in the P-FCS treatment group was markedly upregulated, which suggested that FCS may be activated the NF-*κ*B signaling pathway through TLRs to regulate immune activity. Moreover, the chain conformation of FCSs had been revealed to affect their biological activities [29]. Accordingly, the disparate efficiency between G-FCS and P-FCS confirmed our previous assumption, the bioactivities on fin regeneration, locomotion, and immune response of FCS were presumably determined by the structural characteristics, with the elongated linear chains and higher height of P-FCS molecular might contribute to its stronger function *in vivo*.

Oxidative stress induced following a wound is the main obstacle for wound healing since excessive free radicals around the wound damage the surrounding tissues that cause the retard of wound enclosure [19]. Antioxidase of SOD, CAT, and G6PD had the effects of converting peroxides formed in the body into less toxic and harmless substances and played an important role in keeping the homeostasis of oxidation and dynamic equilibrium of free radicals *in vivo*. SOD was the primary parclose against oxidative damage and could dismutate the superoxide anion radical into hydrogen peroxide (H_2O_2), ulteriorly detoxified H_2O_2 by CAT [49]. G6PD was an enzyme that catalyzes the first reaction in the pentose phosphate pathway, providing reducing power for all cells [50]. FCS isolated from *S. chloronotus*, *Acaudina molpadioidea*, and *A. japonicus* was demonstrated to scavenge free radicals remarkedly, that it can serve as a potent antioxidant *in vitro* [1]. A current study presented that amputation significantly decreased the contents of CAT, SOD, and G6PD, and their levels notably recovered under FCS treatment, suggesting that FCS had antioxidant protection effects on zebrafish larvae following amputation and exerted positive impacts on the restoration of tissues.

5. Conclusion

In conclusion, the G-FCS and P-FCS obtained from green and purple *A. japonicus* are with different molecular weights, and the main discrepancy of structures is the characterization of surface topological features. G-FCS and P-FCS tended to have beneficial effects on caudal fin regeneration of zebrafish at 4–120 hpa, in which 48 hpa was regarded as the key period following FCS treatment associated with the upregulated mRNA expression of Wnt/*β*-catenin, BMP, FGF, and IGF pathways-related genes. Meanwhile, the locomotor activity of amputated larvae was also differently improved. As modulators in the regeneration process, P-FCS functioned at the early stage, while G-PCS in the later stages. It was demonstrated that both FCSs exerted immunomodulatory activity to enhance regeneration via facilitating the secretion of immunomodulatory cytokines, and the immunomodulatory function may be mediated through the promotion of NF-*κ*B and TLRs pathways. In addition, both FCSs also exhibited antioxidant capacity, which could also

prompt the restoration of tissues. These findings would provide the basis for developing drugs to accelerate wound healing and tissue remodeling, and also establish a fundament for further utilization and development of different color morphs of *A. japonicus*.

Data Availability

The data used to support the findings of this study are included in the article and the supplementary information file.

Conflicts of Interest

The authors declare that they have no conflicts of interest.

Acknowledgments

This work was supported by the National Key Research and Development Program of China (2018YFD0901601).

Supplementary Materials

S1 Table: sequences of the primers used in the qRT-PCR experiment. F and R represent forward primer and reverse primer, respectively. (*Supplementary Materials*)

References

[1] J. Mou, Q. Li, X. Qi, and J. Yang, "Structural comparison, antioxidant and anti-inflammatory properties of fucosylated chondroitin sulfate of three edible sea cucumbers," *Carbohydrate Polymers*, vol. 185, pp. 41–47, 2018.

[2] J. H. Kang, K. H. Yu, J. Y. Park, C. M. An, J. C. Jun, and S. J. Lee, "Allele-specific PCR genotyping of the HSP70 gene polymorphism discriminating the green and red color variants sea cucumber (Apostichopus japonicus)," *J Genet Genomics*, vol. 38, no. 8, pp. 351–355, 2011.

[3] Y. Bai, L. Zhang, S. Liu et al., "The effect of salinity on the growth, energy budget and physiological performance of green, white and purple color morphs of sea cucumber, Apostichopus japonicus," *Aquaculture*, vol. 437, pp. 297–303, 2015.

[4] X. J. Sun, Q. Li, and L. F. J. A. Kong, "Comparative mitochondrial genomics within sea cucumber (Apostichopus japonicus): provide new insights into relationships among color variants," *Aquaculture*, vol. 309, no. 1-4, pp. 280–285, 2010.

[5] Y. Khotimchenko, "Pharmacological potential of sea cucumbers," *International Journal of Molecular Sciences*, vol. 19, no. 5, p. 1342, 2018.

[6] N. I. Ibrahim, S. K. Wong, I. N. Mohamed et al., "Wound healing properties of selected natural products," *International Journal of Environmental Research and Public Health*, vol. 15, no. 11, p. 2360, 2018.

[7] L. C. Shanley, O. R. Mahon, D. J. Kelly, and A. Dunne, "Harnessing the innate and adaptive immune system for tissue repair and regeneration: considering more than macrophages," *Acta Biomaterialia*, vol. 133, pp. 208–221, 2021.

[8] A. E. Boniakowski, A. S. Kimball, B. N. Jacobs, S. L. Kunkel, and K. A. Gallagher, "Macrophage-mediated inflammation in normal and diabetic wound healing," *The Journal of Immunology*, vol. 199, no. 1, pp. 17–24, 2017.

[9] S. Barrientos, O. Stojadinovic, M. S. Golinko, H. Brem, and M. Tomic-Canic, "Perspective article: growth factors and cytokines in wound healing," *Wound Repair and Regeneration*, vol. 16, no. 5, pp. 585–601, 2008.

[10] S. Y. Kim and M. G. Nair, "Macrophages in wound healing: activation and plasticity," *Immunology & Cell Biology*, vol. 97, no. 3, pp. 258–267, 2019.

[11] M. Gemberling, T. J. Bailey, D. R. Hyde, and K. D. Poss, "The zebrafish as a model for complex tissue regeneration," *Trends in Genetics*, vol. 29, no. 11, pp. 611–620, 2013.

[12] I. M. Sehring, C. Jahn, and G. Weidinger, "Zebrafish fin and heart: what's special about regeneration?" *Current Opinion in Genetics & Development*, vol. 40, pp. 48–56, 2016.

[13] D. Wehner and G. Weidinger, "Signaling networks organizing regenerative growth of the zebrafish fin," *Trends in Genetics*, vol. 31, no. 6, pp. 336–343, 2015.

[14] T. Hasegawa, C. J. Hall, P. S. Crosier et al., "Transient inflammatory response mediated by interleukin-1β is required for proper regeneration in zebrafish fin fold," *Elife*, vol. 6, Article ID e22716, 2017.

[15] V. Miskolci, J. Squirrell, J. Rindy et al., "Distinct inflammatory and wound healing responses to complex caudal fin injuries of larval zebrafish," *Elife*, vol. 8, Article ID e45976, 2019.

[16] M. Nguyen-Chi, B. Laplace-Builhe, J. Travnickova et al., "TNF signaling and macrophages govern fin regeneration in zebrafish larvae," *Cell Death & Disease*, vol. 8, no. 8, Article ID e2979, 2017.

[17] Z. Julier, A. J. Park, P. S. Briquez, and M. M. Martino, "Promoting tissue regeneration by modulating the immune system," *Acta Biomaterialia*, vol. 53, pp. 13–28, 2017.

[18] X. R. Zhang, C. H. Qi, Y. Guo, W. X. Zhou, and Y. X. Zhang, "Toll-like receptor 4-related immunostimulatory polysaccharides: primary structure, activity relationships, and possible interaction models," *Carbohydrate Polymers*, vol. 149, pp. 186–206, 2016.

[19] J. H. He, Y. P. Liang, M. T. Shi, and B. L. Guo, "Anti-oxidant electroactive and antibacterial nanofibrous wound dressings based on poly(ε-caprolactone)/quaternized chitosan-graft-polyaniline for full-thickness skin wound healing," *Chemical Engineering Journal*, vol. 385, Article ID 123464, 2020.

[20] S. Veeraperumal, H. M. Qiu, S. S. Zeng et al., "Polysaccharides from Gracilaria lemaneiformis promote the HaCaT keratinocytes wound healing by polarised and directional cell migration," *Carbohydrate Polymers*, vol. 241, Article ID 116310, 2020.

[21] Y. Wu, Z. Zhou, L. Luo et al., "A non-anticoagulantheparin-like snail glycosaminoglycan promotes healing of diabetic wound," *Carbohydrate Polymers*, vol. 247, Article ID 116682, 2020.

[22] J. Yang, Y. Wang, T. Jiang, and Z. Lv, "Novel branch patterns and anticoagulant activity of glycosaminoglycan from sea cucumber Apostichopus japonicus," *International Journal of Biological Macromolecules*, vol. 72, pp. 911–918, 2015.

[23] X. T. Fan, T. T. Hou, T. Z. Sun et al., "Starvation Stress Affects the Maternal Development and Larval Fitness in Zebrafish (*Danio rerio*)," *Science of the Total Environment*, vol. 695, Article ID 133897, 2019.

[24] G. Bernardi and G. F. Springer, "Properties of highly purified fucan," *Journal of Biological Chemistry*, vol. 237, no. 1, pp. 75–80, 1962.

[25] M. E. Duarte, M. A. Cardoso, M. D. Noseda, and A. S. Cerezo, "Structural studies on fucoidans from the brown seaweed Sargassum stenophyllum," *Carbohydrate Research*, vol. 333, no. 4, pp. 281–293, 2001.

[26] W. Liu, H. Wang, J. P. Yu et al., "Structure, chain conformation, and immunomodulatory activity of the polysaccharide purified from Bacillus Calmette Guerin formulation," *Carbohydrate Polymers*, vol. 150, pp. 149–158, 2016.

[27] S. Li, J. Li, Z. Zhi et al., "Macromolecular properties and hypolipidemic effects of four sulfated polysaccharides from sea cucumbers," *Carbohydrate Polymers*, vol. 173, pp. 330–337, 2017.

[28] T. M. McIntire and D. A. Brant, "Imaging of carrageenan macrocycles and amylose using noncontact atomic force microscopy," *International Journal of Biological Macromolecules*, vol. 26, no. 4, pp. 303–310, 1999.

[29] X. Xu, C. Xue, Y. Chang, F. Chen, and J. Wang, "Conformational and physicochemical properties of fucosylated chondroitin sulfate from sea cucumber Apostichopus japonicus," *Carbohydrate Polymers*, vol. 152, pp. 26–32, 2016.

[30] Q. Zhu, L. Lin, and M. Zhao, "Sulfated fucan/fucosylated chondroitin sulfate-dominated polysaccharide fraction from low-edible-value sea cucumber ameliorates type 2 diabetes in rats: new prospects for sea cucumber polysaccharide based-hypoglycemic functional food," *International Journal of Biological Macromolecules*, vol. 159, pp. 34–45, 2020.

[31] J. Valcarcel, R. Novoa-Carballal, R. I. Perez-Martin, R. L. Reis, and J. A. Vazquez, "Glycosaminoglycans from marine sources as therapeutic agents," *Biotechnology Advances*, vol. 35, no. 6, pp. 711–725, 2017.

[32] Y. Xie, A. H. Meijer, and M. J. M. Schaaf, "Modeling inflammation in zebrafish for the development of anti-inflammatory drugs," *Frontiers in Cell and Developmental Biology*, vol. 8, Article ID 620984, 2020.

[33] M. Shida, T. Mikami, J. I. Tamura, and H. Kitagawa, "A characteristic chondroitin sulfate trisaccharide unit with a sulfated fucose branch exhibits neurite outgrowth-promoting activity: novel biological roles of fucosylated chondroitin sulfates isolated from the sea cucumber Apostichopus japonicus," *Biochemical and Biophysical Research Communications*, vol. 487, no. 3, pp. 678–683, 2017.

[34] L. Sun, L. Gu, H. Tan et al., "Effects of 17α-ethinylestradiol on caudal fin regeneration in zebrafish larvae," *Science of the Total Environment*, vol. 653, pp. 10–22, 2019.

[35] J. Y. Hong, J. Zapata, A. Blackburn et al., "A catenin of the plakophilin-subfamily, Pkp3, responds to canonical-Wnt pathway components and signals," *Biochemical and Biophysical Research Communications*, vol. 563, pp. 31–39, 2021.

[36] Q. Li, C. Cai, Y. Chang et al., "A novel structural fucosylated chondroitin sulfate from Holothuria Mexicana and its effects on growth factors binding and anticoagulation," *Carbohydrate Polymers*, vol. 181, pp. 1160–1168, 2018.

[37] S. S. Deepa, Y. Umehara, S. Higashiyama, N. Itoh, and K. Sugahara, "Specific molecular interactions of oversulfated chondroitin sulfate E with various heparin-binding growth factors," *Journal of Biological Chemistry*, vol. 277, no. 46, pp. 43707–43716, 2002.

[38] T. Miyazaki, S. Miyauchi, A. Tawada, T. Anada, S. Matsuzaka, and O. Suzuki, "Oversulfated chondroitin sulfate-E binds to BMP-4 and enhances osteoblast differentiation," *Journal of Cellular Physiology*, vol. 217, no. 3, pp. 769–777, 2008.

[39] J. P. Cooke, "Inflammation and its role in regeneration and repair A caution for novel anti-inflammatory therapies," *Circulation Research*, vol. 124, no. 8, pp. 1166–1168, 2019.

[40] S. Balaji, A. King, E. Marsh et al., "The role of interleukin-10 and hyaluronan in murine fetal fibroblast function in vitro: implications for recapitulating fetal regenerative wound healing," *PLoS One*, vol. 10, no. 5, Article ID e0124302, 2015.

[41] H. Wang, L. Xu, M. Yu et al., "Glycosaminoglycan from Apostichopus japonicus induces immunomodulatory activity in cyclophosphamide-treated mice and in macrophages," *International Journal of Biological Macromolecules*, vol. 130, pp. 229–237, 2019.

[42] S. Jiang, H. Yin, X. Qi et al., "Immunomodulatory effects of fucosylated chondroitin sulfate from Stichopus chloronotus on RAW 264.7 cells," *Carbohydrate Polymers*, vol. 251, Article ID 117088, 2021.

[43] D. M. Mosser and J. P. Edwards, "Exploring the full spectrum of macrophage activation," *Nature Reviews Immunology*, vol. 8, no. 12, pp. 958–969, 2008.

[44] I. Arundina, Y. Yuliati, P. Soesilawati, D. W. Damaiyanti, and D. Maharani, "The effects of golden sea cucumber extract (Stichopus hermanii) on the number of lymphocytes during the healing process of traumatic ulcer on wistar rat's oral mucous," *Dental Journal*, vol. 48, no. 2, p. 100, 2015.

[45] I. A. Schepetkin and M. T. Quinn, "Botanical polysaccharides: macrophage immunomodulation and therapeutic potential," *International Immunopharmacology*, vol. 6, no. 3, pp. 317–333, 2006.

[46] T. Kawai and S. Akira, "TLR signaling," *Cell Death & Differentiation*, vol. 13, no. 5, pp. 816–825, 2006.

[47] S. Ntoufa, M. G. Vilia, K. Stamatopoulos, P. Ghia, and M. Muzio, "Toll-like receptors signaling: a complex network for NF-κB activation in B-cell lymphoid malignancies," *Seminars in Cancer Biology*, vol. 39, pp. 15–25, 2016.

[48] H. Suga, M. Sugaya, H. Fujita et al., "TLR4, rather than TLR2, regulates wound healing through TGF-β and CCL5 expression," *Journal of Dermatological Science*, vol. 73, no. 2, pp. 117–124, 2014.

[49] M. Schäfer and S. Werner, "Oxidative stress in normal and impaired wound repair," *Pharmacological Research*, vol. 58, no. 2, pp. 165–171, 2008.

[50] M. D. Cappellini and G. Fiorelli, "Glucose-6-phosphate dehydrogenase deficiency," *The Lancet*, vol. 371, no. 9606, pp. 64–74, 2008.